Global radius-of-curvature estimation and control for the Hobby-Eberly Telescope

Rakoczy, John, Hall, Drew, Ly, William, Howard, Richard, Montgomery, Edward

John M. Rakoczy, Drew Hall, William Ly, Richard T. Howard, Edward E. Montgomery IV, "Global radius-of-curvature estimation and control for the Hobby-Eberly Telescope," Proc. SPIE 4837, Large Ground-based Telescopes, (4 February 2003); doi: 10.1117/12.456650

SPIE.

Event: Astronomical Telescopes and Instrumentation, 2002, Waikoloa, Hawai'i, United States

Global radius-of-curvature estimation and control for the Hobby-Eberly Telescope

John Rakoczy, Drew Hall, William Ly, Ricky Howard, Edward Montgomery
NASA Marshall Space Flight Center
Huntsville, Alabama

ABSTRACT

A system which estimates the global radius of curvature (GRoC) and corrects for changes in GRoC on a segmented primary mirror has been developed for and verified on McDonald Observatory's Hobby Eberly Telescope (HET). The GRoC estimation and control system utilizes HET's primary mirror control (PMC) system and the Segment Alignment Maintenance System (SAMS), an inductive edge sensor system. A special set of boundary conditions is applied to the derivation of the optimal edge-match control. The special boundary conditions allow the further derivation of an observer, which enables estimation and control of the GRoC mode to within HET's specification. The magnitude of the GRoC mode can then be controlled despite the inability of the SAMS edge sensor system, by itself, to observe or control the GRoC mode. The observer can be extended to any segmented mirror telescope. It will be shown that the observer improves with accuracy as the number of segments increases. This paper presents the mathematical theory of the observer. Performance verification data from the HET will be presented.

Keywords: segmented mirror, radius-of-curvature, edge sensors, active optics

INTRODUCTION

In October 2000, a prototype of the Segment Alignment Maintenance System (SAMS) was installed on a 7-segment sub-array of the Hobby-Eberly Telescope (HET). The SAMS utilized inductive edge sensors to sense the tip, tilt and piston errors of the HET segments from their reference positions [1]. Since the inductive edge sensor architecture was insensitive to the Global Radius of Curvature (GRoC) mode of the primary mirror, the MSFC and Blue Line Engineering team conceived a configuration of inclinometers that would, in theory, provide sufficient dihedral angle information in order to sense changes in the GRoC mode. Subsequent testing revealed that the best off-the-shelf inclinometers available at the time did not have adequate temperature stability, nor did they have adequate scale factor stability over the expected dynamic range. Consequently, the inclinometers were removed from the optimal control matrix, and the Sub-array Test proceeded with the GRoC mode left uncontrolled. Sub-array Test results indicated that SAMS performance was unacceptable without some way of sensing and correcting GRoC mode changes due to the coupling of the edge-matching control system with boundary condition motion[2].

The optimal edge-matching control for the Sub-array Test was derived by imposing 4 constraints or boundary conditions on the mathematical optimization problem. Figure 1 shows the layout of the segments in the Sub-array Test. The shaded segments were mathematically constrained in their piston degrees-of-freedom in order to derive a unique optimal edge-matching control gain matrix. Each 'x' denotes the active edge sensor coils. Each 'o' denotes the passive or target sensor coils. The numbers on the segments are in accord with the numbering system defined for the Hobby-Eberly Telescope.

Large Ground-based Telescopes, Jacobus M. Oschmann, Larry M. Stepp, Editors,
Proceedings of SPIE Vol. 4837 (2003) © 2003 SPIE · 0277-786X/03/$15.00

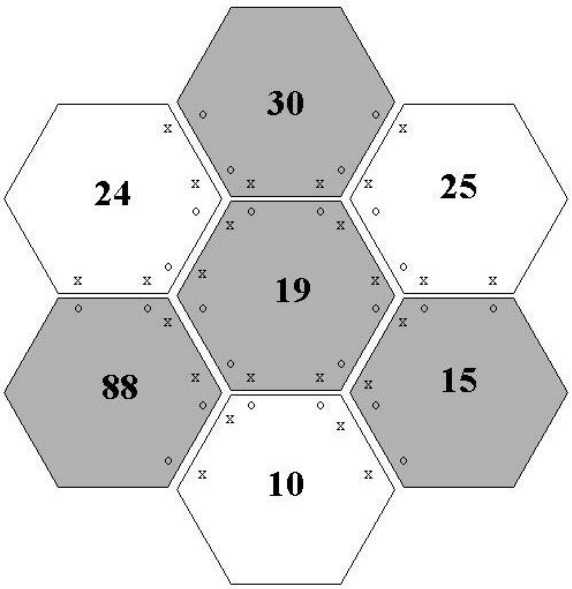

Figure 1: SAMS Sub-Array Test layout on Hobby-Eberly Telescope

The boundary condition segments can be thought of as four non-collinear points in three-dimensional space. The four non-collinear points define a reference sphere. If any or all of the coordinates of the four points change in 3-dimensional space, the motion changes the shape and orientation of the sphere the four points define.

The control system was derived to minimize the global variance of the edge shear errors subject to the constraint that the four prescribed segments do not move in their piston degrees-of-freedom. This way the control system maintains edge continuity on the reference sphere while the four boundary condition segments stay fixed. However, one cannot expect that the boundary condition segments do not move in piston. Boundary condition piston motion drives the control system to match up segment edges to fit a different sphere than the reference sphere. In fact, since the control system corrects all other modes of the primary mirror, the only way the primary mirror's sphere can change is by the control system changing its shape subject to motion of the boundary condition segments.

The impetus for the GRoC estimator came from the thought that if the control system is the only thing driving the change in GRoC, one can use the control system command time history to estimate the shape of the sphere induced by boundary condition motions. In particular, the accumulated moves executed by the control system since setting the current edge sensor reference indicate the shape of the sphere to which the control system has driven the primary mirror.

In June 2001, a GRoC estimator was derived and applied *ex post facto* to data archived from the SAMS 7-segment Sub-array Test. The GRoC-mode corrections calculated by the GRoC estimator were compared with the manual GRoC adjustments made during the Sub-array test. The results indicated that about 80 percent of the time the GRoC estimator computed the correct GRoC adjustment with an error tolerance within HET's specification[3]. That analysis also showed that the estimator always got the correct sign on the direction of the GRoC mode. Those results showed that the GRoC estimator concept was feasible and merited extension to the full 91-segment array. Full-array SAMS installation was completed in October 2001, and the GRoC estimator software was installed and verified on the full array in December 2001.

This paper describes the theory, implementation and verification of a global radius of curvature estimation and control system for the Hobby-Eberly Telescope. The first section details the mathematical theory of the GRoC

estimator. The theory shows how the 4-point constraint architecture yields influence function and control system matrices with special properties. The special properties were exploited in order to derive an accurate full-state estimator. The first section quantifies the inherent error in the estimator and shows how the estimator improves with accuracy as the number of segments increases. The second section describes how the estimator matrix is integrated with the edge sensor control system to realize a complete Global Radius of Curvature Estimation and Control System (GRoCECS). The third section presents results of verification testing performed on the Hobby-Eberly Telescope in December 2001. The verification data validate the theory and prove that the GRoCECS can be used to accurately control a segmented mirror's GRoC mode.

SECTION 1: MATHEMATICAL THEORY OF GROC ESTIMATOR

The general influence function relating all tip, tilt and piston degrees of freedom (also referred to as states) to edge sensor outputs is the following:

$$e = C_{480x273} x_{273x1} \tag{1.1}$$

The vector e comprises all 480 edge sensor measurements. The vector x comprises all 273 tip, tilt and piston degrees of freedom or states of the primary mirror. The matrix $C_{480x273}$ is the full-array influence matrix. The 480 edge sensors were installed on the primary mirror in the same pattern as for the Sub-array test, shown in Figure 1 above. The edge sensor layout pattern in Figure 1 was extended to 5 rings of hexagons. Figure 2 shows the layout of all 91 segments, 5 rings, on the Hobby-Eberly Telescope.

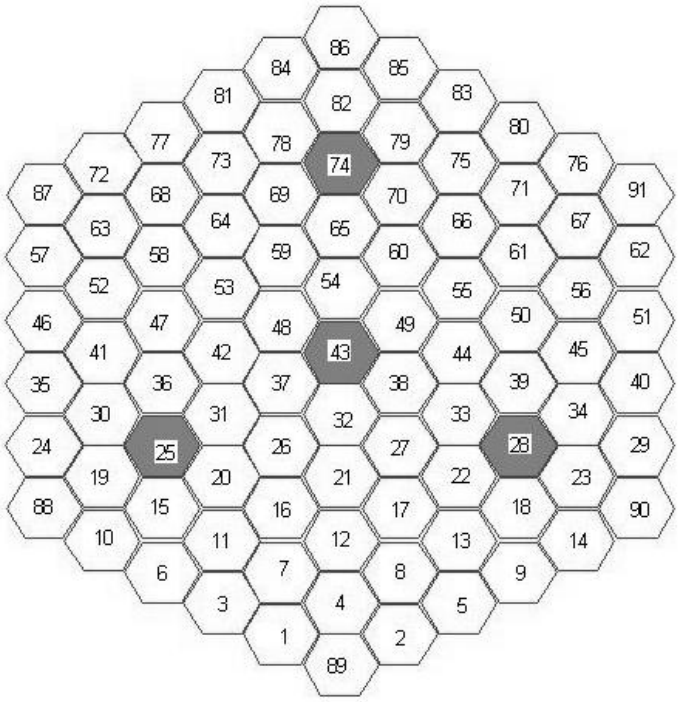

Figure 2: HET segment layout with SAMS boundary conditions

When the four boundary condition constraints are imposed, one obtains a diminished influence matrix $C_{480x269}$. The four piston boundary conditions are on the shaded segments shown in Figure 2. The optimal control system gains are computed from the modified influence matrix according to the following equation:

$$K = (C^T_{480\,x\,269} C_{480\,x\,269})^{-1} C^T_{480\,x\,269} \tag{1.2}$$

Thus, control gain matrix K is the pseudoinverse of the modified influence matrix $C_{480x269}$. $C_{480x269}$ is full rank, so ($C_{480x269}{}^T C_{480x269}$) is invertible. The dimension of K is 269x480. Then the control command to the 269 active degrees of freedom is the following:

$$u_{269\,x1} = K(e_{ref} - e) \tag{1.3}$$

The vector e_{ref} constitutes the edge sensor measurements taken when the mirror was aligned to the position yielding the best possible image quality. Those edge sensor measurements are the reference measurements. Equations 1.1 - 1.3 establish the open-loop and closed-loop relations between the states, the edge sensor measurements, and the control commands. It is next advantageous to investigate the closed-loop influence function from a state vector x to the control command u. Combining equations 1.1-1.3 yields

$$u_{269\,x1} = KC_{480\,x273}(x_{ref} - x)_{273\,x1} \tag{1.4}$$

The closed-loop influence matrix, Q, is defined by the following equation:

$$Q = KC_{480\,x\,273} \tag{1.5}$$

The closed-loop influence matrix, Q, has dimension 269x273. Q maps dynamic perturbations in the states x to control commands in u. There is not a one-to-one mapping of each perturbation in x into a corresponding control motion in u. In fact, boundary condition perturbations in x map to GRoC-mode motions in u. This relationship provides the mathematical nomenclature to fit the qualitative description given earlier in the introduction as to how boundary condition motions induce changes in shape and orientation of the reference sphere. Deeper scrutiny of Q reveals that Q has a special mathematical quality as shown in equation 1.6.

$$Q = \left(-I \mid q\right) \tag{1.6}$$

Equation 1.6 shows that Q can be partitioned into two sub-matrices. The first partition is simply the negative of the identity matrix of dimension 269x269. The first partition simply maps disturbances in each active degree of freedom to the same value, except negative, in the control. The mathematics describes the negation of the sensed disturbance, which is what closed-loop control is supposed to do. The second partition, q, is a matrix with dimension 269x4. The columns of q are each a GRoC-mode vector which the control system responds with when the boundary condition degrees of freedom are perturbed. Note also that Q has rank equal to 269.

After having described all the open-loop and closed-loop relationships, it is time to use the relationships in estimating the parameters that will help compensate for controller-induced changes in GRoC. Equation 1.4 seems to imply that one could estimate the perturbations in x by performing a pseudo-inverse of Q and multiplying it to the control commands u. If one accumulates all past control commands, one can apply the pseudo-inverse to estimate the accumulated perturbations to the states x.

$$Q^+ \sum u_{269\,x1} = Q^+ Q \sum \Delta\hat{x}_{273\,x1} \tag{1.7}$$

Q^+ is the pseudoinverse of Q. The pseudoinverse of Q was evaluated by singular value decomposition (SVD) because Q^TQ, which has dimension 273x273, has rank of only 269. Thus Q^TQ is not invertible, and the classic pseudo-inverse formula, exploited in equation 1.2, cannot be utilized in this situation. If Q^TQ were full rank, then a unique least-squares solution could be obtained, and the following equations would hold:

$$Q^+Q = I, \tag{1.8}$$

$$Q^+ \sum u_{269x1} = \sum \Delta\hat{x}_{273x1} \tag{1.9}$$

Thus, if Q^TQ were full rank, then Q^+Q would be the identity matrix, I. However, this is not the case. If Q^+Q were very close to the identity matrix, then one could assert:

$$Q^+ \sum u_{269x1} \cong \sum \Delta\hat{x}_{273x1} \tag{1.10}$$

Equation 1.10 then yields an approximate estimate of all states in x. More precisely, equation 1.10 gives an estimate of the accumulated closed-loop motions of the controlled degrees of freedom, and it gives an estimate of the accumulated open-loop motions of the four uncontrolled degrees-of-freedom. The states of most particular interest are the states corresponding to the uncontrolled piston degrees of freedom of the four boundary condition segments. The quality and accuracy of the estimates depend on how closely Q^+Q approximates the identity matrix. A good figure of merit for determining how closely one is to the identity matrix is the root-mean-square (RMS) of the diagonal elements of the error matrix E. The error matrix E is expressed in equation 1.11. Table 1 tabulates the figure of merit for five conceivable configurations of hexagonally segmented primary mirrors.

$$E = I - Q^+Q \tag{1.11}$$

Note that for a single ring of hexagonal mirror segments, the anticipated error in the estimates is 20 percent. Observe that the ratio of null space vectors to the larger dimension of the Q matrix is 4/21, approximately 20 percent. Recall from the introduction section that the GRoC estimator preliminary analysis, using 7-segment sub-array test data, indicated that the estimator was correct about 80 percent of the time while always getting the correct sign. The results in Table 1 illuminate the source of the estimator error in the 7-segment configuration.

Looking at Table 1, observe how the error term gets smaller as the number of rings and the number of segments increase. The error appears to decline asymptotically. At five rings and 91 segments, the full-array HET, the error term is only 2 percent. The ratio of null space vectors to the large dimension in the 5-ring case is 4/273, approximately 1.5 percent. The trends in Table 1 suggest that as Q^+Q approaches, in the limit, a square, full-rank matrix, the error in the estimator, in the limit, goes to zero. Table 1 indicates that the estimator realized in equation 1.10 yields estimates of all tip, tilt and piston states (including the boundary condition states) with about only 2 percent inherent residual error on the full-array HET.

Rings	Segments	Size(Q)	Rank(Q)	RMS(diag(I-Q^+Q))
1	7	17 x 21	17	0.20
2	19	53 x 57	53	0.08
3	37	107 x 111	107	0.04
4	61	179 x 183	179	0.03
5	91	269 x 273	269	0.02

Table 1: GRoC estimator inherent error vs. number of rings and segments

SECTION 2: GROCECS IMPLEMENTATION

This section describes the functional implementation of the GRoCECS. Figure 3 illustrates the data flow within the combined SAMS/GRoCECS. The combined SAMS/GRoCECS consists of two separate entities, the edge sensor control system and the GRoC estimator, which are tied together in the SAMS software[4,5]. The edge sensor control system accepts edge sensor measurements and edge sensor reference values as its inputs and outputs actuator motion commands. The GRoC estimator accepts actuator commands as inputs and outputs edge sensor reference values to the edge sensor control system.

There were two options for implementing the GRoC corrections in the SAMS system. One option was to estimate the boundary condition segment piston motions and negate them with piston motion commands to the segments. However, the HET's mirror/actuator/mount assembly cannot be trusted for accurate, repeatable open-loop motion commands. Testing has shown that actual motions vary from 60 percent to 130 percent of the commanded motion. There was just too much error in the move commands to apply this approach. Significant errors in the positioning of the boundary condition segments would define the wrong reference sphere to which the edge sensor control loop would match up the edges. This would defeat the whole purpose of correcting for the array's converging to the wrong reference sphere.

A second option was to use the boundary condition piston motion estimates as bias commands to the edge sensor control loop. Since the SAMS closed-loop is limited only by the noise in the edge sensors (< 30 nanometers RMS), using the SAMS closed-loop to adjust the boundary condition positions was judged to be much more reliable than open-loop mirror motions. Under this scenario, the GRoC estimator computes the estimated boundary condition piston motions. The piston motions are then converted to equivalent edge sensor readings of what the edge s ensors surrounding that segment would see if that segment had pistoned that much above or below the rest of the array. The equivalent sensor values are used as biases to the edge-matching control system error signals. Under this approach, if the estimator senses that a boundary condition segment has pistoned, it sends biases to the edge-matching control loop to prevent that loop from matching up segment edges to the wrong reference sphere. A side-effect of this approach is that boundary condition segments will stand out above or below the rest of the array. Since the HET's requirements do not require segment phasing, (The piston maintenance requirement is 15 microns RMS) segments protruding from the array by a few microns will not adversely affect telescope performance.

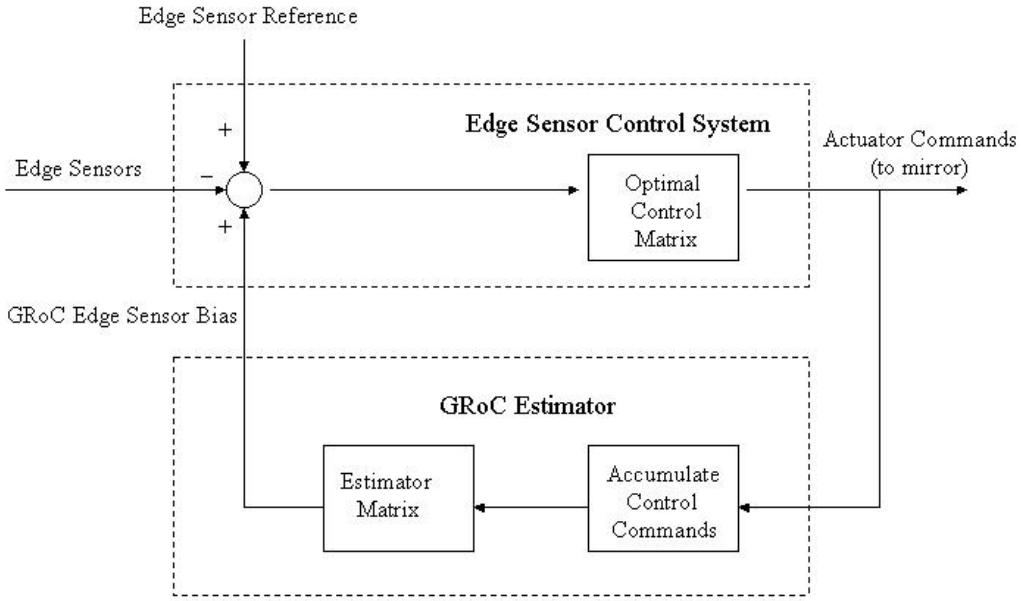

Figure 3: Conceptual Operation of GRoCECS

The edge sensor control system consists of the following matrix equation:

$$u = K(e_{reference} - e + e_{groc\_bias}) \tag{2.1}$$

The vector u contains all the actuator commands for all mirror degrees of freedom except for the four prescribed boundary conditions. The vector u nominally has dimension 269x1. The vector $e_{reference}$ contains all edge sensor measurements recorded when the mirror reference was set. The vector e contains all the edge sensor measurements at the current sample interval. The vector e_{groc_bias} contains all the edge sensor biases computed by the GRoC estimator on the last iteration. Nominally, the edge sensor measurement and reference vectors have dimension 480x1. The matrix K is the optimal edge sensor control matrix and has a nominal dimension of 269x480. The edge sensor error signal, comprised of the reference, the current measurements, and the GRoC estimator biases, is multiplied by the control matrix K to obtain the mirror actuator commands in u.

Besides being sent to the mirror actuators, the command vector u is sent to the GRoC estimator software. The first thing the GRoC estimator software does is adds the current actuator commands at time interval k to the accumulated commands updated at the last interval k-1. Equation 2.2 shows the summation operation:

$$\sum u_k = \sum u_{k-1} + u_k \tag{2.2}$$

After the summation is complete, the accumulated control commands are input to the estimator matrix in order to calculate the GRoC-based edge sensor biases to the edge sensor control system. Figure 4 shows the flow internal to the GRoC estimator.

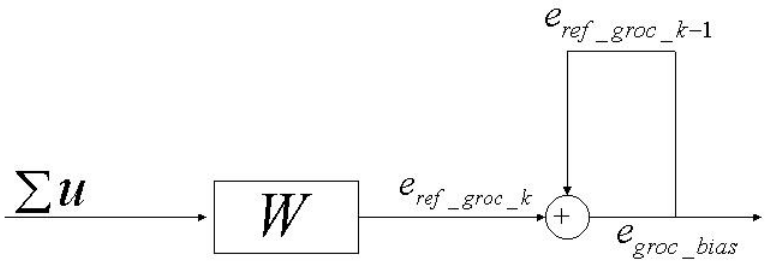

Figure 4: GRoC estimator internal data flow

The first operation in Figure 4 involves multiplying the estimator matrix W by the accumulated commands at interval k. Equation 2.3 describes this operation:

$$e_{ref\_groc\_k} = W(\sum u)_k \tag{2.3}$$

The GRoC estimator matrix, W, is defined in equation 2.4. The matrix W is constructed by premultiplying the pseudoinverse of the closed-loop influence matrix, Q, by the full-array open-loop influence matrix, $C_{480x273}$. This operation converts the state estimates of equation 1.10 into a set of biases for the edge sensor control system.

$$W = -C_{480x273}Q^{+} \tag{2.4}$$

The output vector $e_{ref\_groc\_k}$ is an intermediate edge sensor bias value which corresponds to the change in GRoC since the last data interval k-1. The intermediate bias is then added to the accumulated GRoC-based edge sensor bias in equation 2.5.

$$e_{groc\_bias} = e_{ref\_groc\_k} + e_{ref\_groc\_k-1} \tag{2.5}$$

The vector e_{groc_bias} is the edge sensor bias that is added to the edge sensor error signal in the edge sensor control loop. After the bias is updated, the bias at interval k is assigned to $e_{ref\_groc\_k-1}$ for the next cycle of the loop:

$$e_{ref\_groc\_k-1} = e_{groc\_bias\_k} \tag{2.6}$$

SECTION 3: GROCECS VERIFICATION ON THE HOBBY-EBERLY TELESCOPE

GRoCECS performance was verified in testing conducted December 1-5, 2001 at McDonald Observatory on the Hobby-Eberly Telescope (HET). The equations and flow diagrams described in Sections 1 and 2 were incorporated into the SAMS software.

In Figure 2, segments 43, 74, 25 and 28 were prescribed as the boundary conditions for the edge sensor control system and for the GRoC estimator. The verification testing was conducted in two parts. The first part was a test in which the edge sensor control system operated, but the GRoC estimator was not operational. This test was a baseline test to observe how the radius of curvature changed without the estimator active in the loop. The second test involved the entire GRoCECS being operational to verify its actual performance.

The same experimental procedure was followed for each test. The telescope operator commanded segment 43 to move in its piston degree of freedom in 2-micron increments. After each 2-micron move, the control system was allowed to settle out any transients, and the telescope operator then measured the change in the position of the telescope's focus using instruments in the Center of Curvature Alignment System (CCAS) tower. The telescope operator commanded segment 43 to positions of +2, +4, +6, and +8 microns. The telescope operator then moved segment 43 back to +6, +4, +2, and zero microns (home). Theory predicted that, with the GRoCECS inactive, the focus position would change approximately 300 microns per every 2 microns of piston in segment 43. When the GRoCECS is active, the focus position should not change, or its change should remain within the HET's tolerance for GRoC (+/- 300 microns).

Figure 5 shows the results of the two tests. The data points identified by the "x" and the "o" are the data taken when the GRoCECS was not active. The estimator-off test yields a slope of approximately 375 microns focus change per 2 microns of segment 43 piston motion. The "*" and the "+" identify the data points taken when the GRoCECS was activated. The estimator-on forward test has virtually no slope, while the estimator-on backward test yields at most a slope of –150 microns focus change per 2 microns of segment 43 motion. Note that the direction of the slope was reversed from the estimator-off test, indicating that the GRoCECS had either overcompensated for GRoC changes or the alignment tower was moving slightly. Nevertheless, the estimator-on test maintained the GRoC to within +/- 300 microns of the reference position.

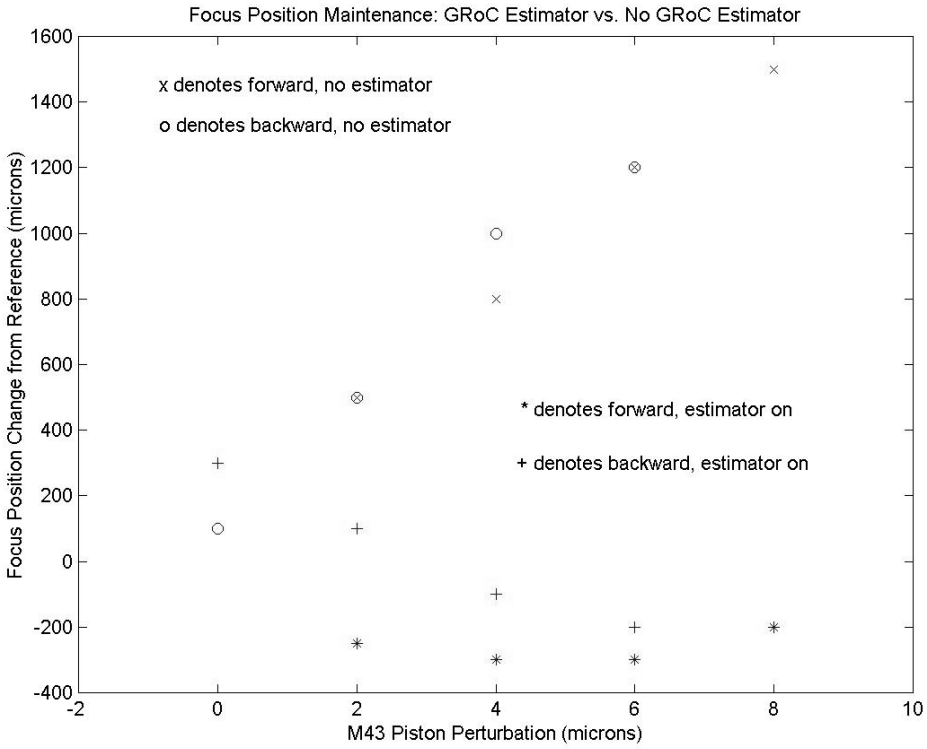

Figure 5: Focus position change during performance verification test

The focus position change test was a good test to indicate whether or not the GRoCECS had actually affected the telescope's ability to maintain focus at the correct radius of curvature. The focus position data are best at telling what the performance is like when the GRoC mode is subject to large disturbances. Errors in focus position metrology as well as errors in open-loop commanding segment 43 motions contribute greatly to the ability to measure the focus position accurately. The ability to measure focus position had, at best, an accuracy of +/- 100 microns. Another figure of merit for evaluating the GRoCECS performance is to compare what the estimator actually estimated segment 43's motions to be versus what the edge sensors actually measured its motion was. Data of this nature would truly prove the GRoCECS's ability as a full-state estimator and controller, especially since the edge sensors are accurate to better than 50 nanometers. Figure 6 is a plot of what the estimator estimated segment 43's piston motion to be. Figure 7 shows the mean of the actual measurements from the edge sensors surrounding segment 43.

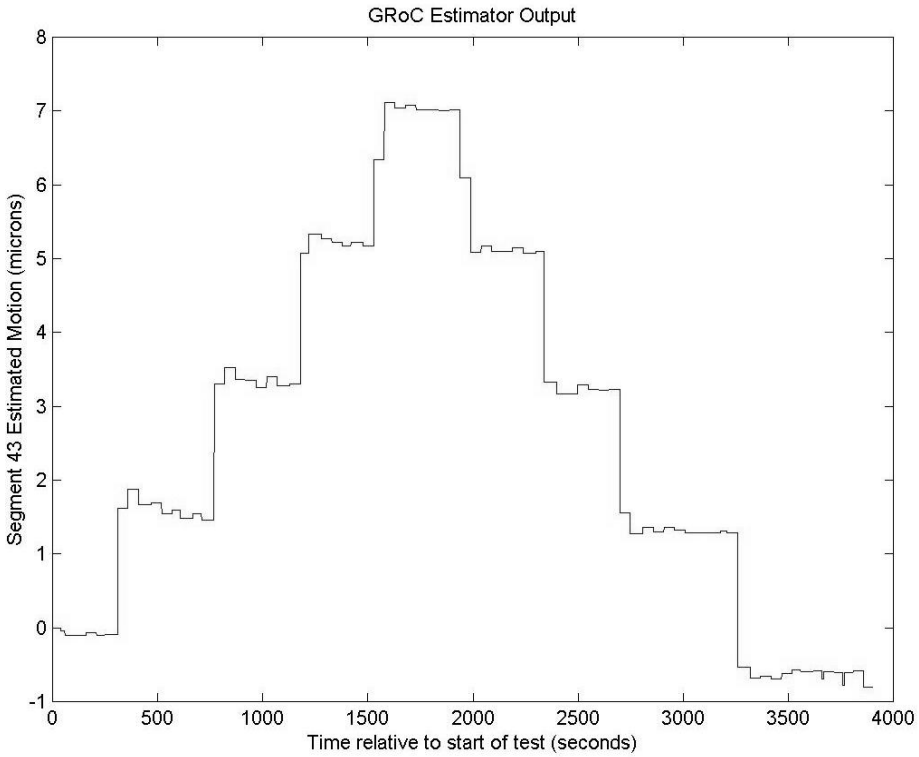

Figure 6: GRoCECS estimate of segment 43 motion

The estimator very precisely compares with the edge sensor outputs. Note that the edge sensors indicate that segment 43 moved in piston by about 1.75 microns per step even though the telescope operator had commanded 2 microns per step. The discrepancy arises from the fact that, on HET, when segments are moved open-loop, they don't go precisely where they are commanded to go. The edge sensor outputs in Figure 7 show a small transient at the start of every commanded step. The transient originates from the fact that the segment's commanded motion and edge-matching control system response are much faster than the GRoC estimator loop. Upon the TO's executing the segment 43 piston move, the edge sensors detect the relative motion. Next, the edge-matching control system tries to negate the disturbance and maintain edge continuity by opening up the sphere so that the edges match up

with segment 43's new position. At this point the edge error readings go back down to where they started. After the GRoC estimator calculates that the edge-matching control system has put a GRoC mode into the mirror, the GRoC estimator sends the biases to the edge sensor loop to negate the GRoC mode. Then the control system contracts the sphere, leaving segment 43 sticking out by the amount the TO had commanded, but the net GRoC change is zero.

As Figure 7 shows, as soon as the estimator catches up and settles, it is very accurate. The data in Figure 6 were subtracted from the data in Figure 7 to calculate the error in the real-time estimate. The RMS error during the time intervals after the transient had settled out was 34 nanometers, which is approximately 2 percent of the motion the TO prescribed for segment 43. The 2 percent error agrees with the prediction for a 5-ring segmented mirror shown in Table 1.

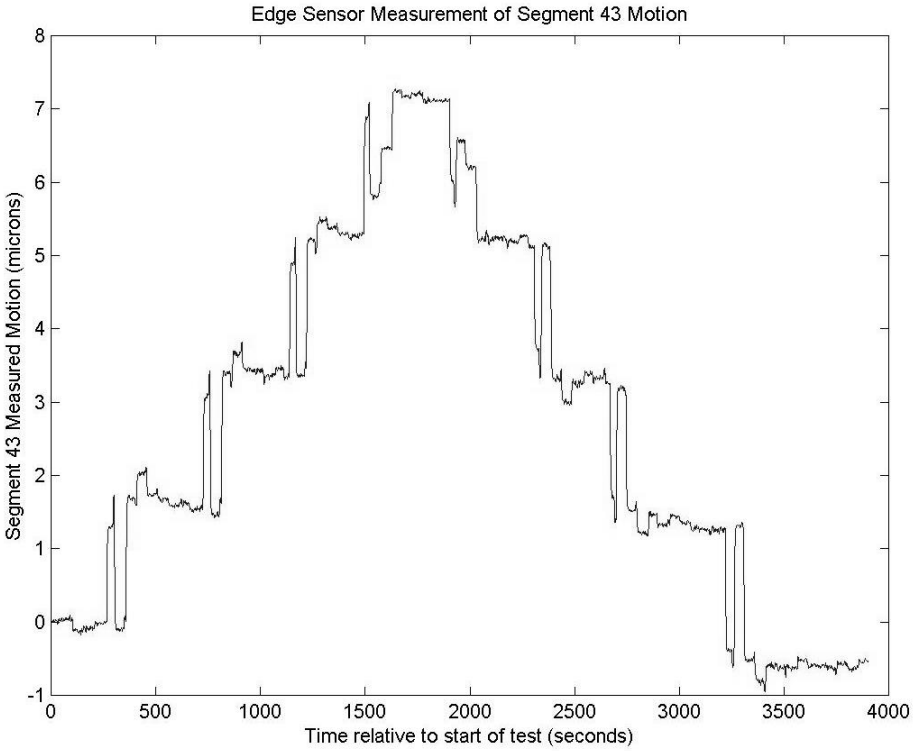

Figure 7: Edge sensor measurement of segment 43 motion

CONCLUSION

A global radius of curvature estimation and control system (GRoCECS) has been developed for the Hobby-Eberly Telescope. Usiing a typical edge sensor architecture that is insensitive to the GRoC mode and a special set of optimal control boundary conditions, the GRoCECS is able to estimate and control the GRoC mode with an inherent error of only two percent. The GRoCECS can be applied to any segmented mirror with similar edge sensor architectures as the HET. The GRoCECS may be implemented by commanding biases to the edge sensor error signals (as on HET), or, alternatively, the GRoCECS could be used to estimate boundary condition segment piston motions and directly control those degrees of freedom. The mathematical theory illuminates another special feature of the GRoCECS. That feature is that the GRoCECS improves in accuracy, as a full-state estimator, as the number of segments increases. The GRoCECS was integrated with the Segment Alignment Maintenance System on HET in

December 2001. Testing on HET verified that the GRoCECS performs in accord with the predictions of the mathematical theory.

REFERENCES

1. J. Booth, M. Adams, G. Ames, J. Fowler, E. Montgomery, J. Rakoczy, "Development of the Segment Alignment Maintenance System (SAMS) for the Hobby-Eberly Telescope," *Optical Design, Materials, Fabrication, and Maintenance*, SPIE **4003**, No. 20, Munich, Germany, March 27-31, 2000.
2. J. Rakoczy, D. Hall, R. Howard, J. Weir, E. Montgomery, G. Ames, T. Danielson, P. Zercher, "Demonstration of a Segment Alignment Maintenance System on a seven-segment sub-array of the Hobby-Eberly Telescope," *Adaptive Optics Systems and Technology II*, SPIE **4494**, pp. 69-80, San Diego, California, July 30 – August 1, 2001.
3. J. Rakoczy, "Preliminary Assessment of a Global Radius of Curvature Estimator for the Hobby-Eberly Telescope," NASA Internal Memo No. SD71-004-01, July 16, 2001.
4. J. Rakoczy, D. Hall, R. Howard, W. Ly, J. Weir, E. Montgomery, M. Adams, J. Booth, J. Fowler, G. Ames, "Primary mirror figure maintenance of the Hobby-Eberly Telescope using the Segment Alignment Maintenance System," *Large Ground-Based Telescpes*, SPIE **4837**, No. 81, Waikoloa, Hawaii, August 21-28, 2002.
5. D. Hall, W. Ly, R. Howard, J. Weir, J. Rakoczy, "Software development for the Hobby-Eberly Telescope's Segment Alignment Maintenance System using LabVIEW," *Advanced Telescope & Instrumentation Control Software II*, SPIE **4848**, No. 25, Waikoloa, Hawaii, August 21-28, 2002.